Environmental Science & Technology
Article
pubs.acs.org/est

Comparison of Hygroscopicity, Volatility, and Mixing State of Submicrometer Particles between Cruises over the Arctic Ocean and the Pacific Ocean

Gibaek Kim,[†] Hee-joo Cho,[†] Arom Seo,[†] Dohyung Kim,[†] Yeontae Gim,[‡] Bang Yong Lee,[‡]
Young Jun Yoon,*[,‡] and Kihong Park*[,†]

[†]National Leading Research Laboratory, School of Environmental Science and Engineering, Gwangju Institute of Science and Technology (GIST), 123 Cheomdangwagi-ro, Buk-gu, Gwangju 61005, Republic of Korea

[‡]Korea Polar Research Institute, 26 Songdomirae-ro, Yeonsu-Gu, Incheon 406-840, Republic of Korea

S Supporting Information

ABSTRACT: Ship-borne measurements of ambient aerosols were conducted during an 11 937 km cruise over the Arctic Ocean (cruise 1) and the Pacific Ocean (cruise 2). A frequent nucleation event was observed during cruise 1 under marine influence, and the abundant organic matter resulting from the strong biological activity in the ocean could contribute to the formation of new particles and their growth to a detectable size. Concentrations of particle mass and black carbon increased with increasing continental influence from polluted areas. During cruise 1, multiple peaks of hygroscopic growth factor (HGF) of 1.1−1.2, 1.4, and 1.6 were found, and higher amounts of volatile organic species existed in the particles compared to that during cruise 2, which is consistent with the greater availability of volatile organic species caused by the strong oceanic biological activity (cruise 1). Internal mixtures of volatile and nonhygroscopic organic species, nonvolatile and less-hygroscopic organic species, and nonvolatile and hygroscopic nss-sulfate with varying fractions can be assumed to constitute the submicrometer particles. On the basis of elemental composition and morphology, the submicrometer particles were classified into C-rich mixture, S-rich mixture, C/S-rich mixture, Na-rich mixture, C/P-rich mixture, and mineral-rich mixture. Consistently, the fraction of biological particles (i.e., P-containing particles) increased when the ship traveled along a strongly biologically active area.

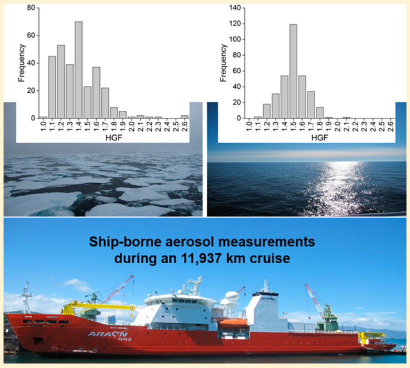

INTRODUCTION

Oceans cover the majority (over 70%) of the earth's surface, and marine aerosols are one of the largest global contributors to the ambient atmospheric aerosols (1300−3300 Tg/yr globally).[1,2] Variation of the concentration and properties of marine aerosols can cause significantly different direct (radiation balance) and indirect (cloud formation) effects on the climate system.[3−5] Marine aerosols originating from the ocean in the marine boundary layer (MBL) are typically produced by a bubble bursting process from the surface of seawater (i.e., primary marine aerosols or sea spray aerosols (SSA)) and by gas-to-particle conversion of gaseous compounds emitted from seawater (i.e., secondary marine aerosols). Thus, the properties of seawater are also important parameters to determine the physical and chemical properties of marine aerosols.[6,7]

The chemical components and mixing state of marine aerosols typically vary with size.[8] Sea salts (produced by a bubble bursting process) are known to be the major chemical component of marine aerosols, especially those larger than 1 μm, while mixtures of sea salts, nonsea salt (nss)-sulfates, and organics are abundant in the submicrometer size range.[2,9,10] The nss-sulfates can be produced by a gas-to-particle conversion process (secondary). The dependence of a significant portion of the organic fraction in the submicrometer marine aerosols (30−65%) on biological activity in seawater was reported.[10−12] The organic fraction of aerosols over the northeast Pacific Ocean decreased with increasing size, ranging from 7% to 25% in the fine mode, while sea salt was dominant in the coarse mode (~70%) and rare in the fine mode.[13] Their chemical data on submicrometer particles in the MBL suggest that the organic fraction mostly consists of di- and polycarboxylic acids.[13] However, the amount of the organic fraction and how its components mix with inorganic species in size-resolved submicrometer particles have not been definitively determined.

The long-range transport of natural (e.g., dust) and anthropogenic aerosols from continents can also affect the chemical composition and mixing states of aerosols observed over the ocean (i.e., continental aerosols can be mixed with marine aerosols originating from the ocean including both primary and secondary aerosols).[14−16] The bulk analysis of

Received: April 1, 2015
Revised: September 10, 2015
Accepted: September 21, 2015
Published: September 21, 2015

DOI: 10.1021/acs.est.5b01505
Environ. Sci. Technol. 2015, 49, 12024−12035

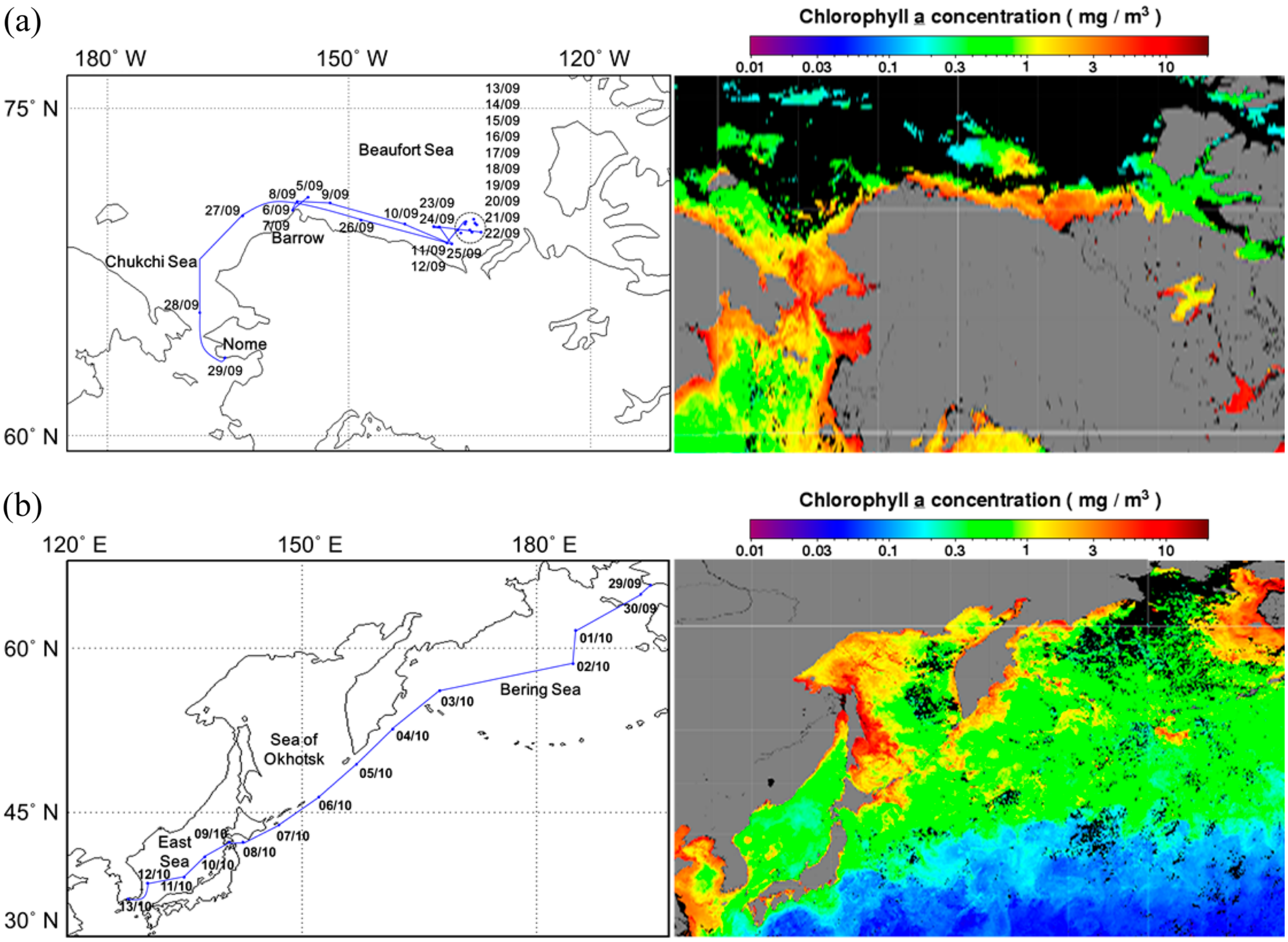

Figure 1. Ship tracks (a) over the Arctic Ocean (9/7/2013−9/29/2013) and (b) over the Pacific Ocean (9/29/2013−10/13/2013) with chlorophyll-a concentration in September and October in 2013 (satellite data were obtained from http://oceancolor.gsfc.nasa.gov/). The blacked out area was displayed when the chlorophyll-a data from satellite were not available due to sea ice, cloud, etc.

aerosols, which assumes that all particles are internal mixtures of multiple components, may misleadingly indicate that all particles have the same potential for cloud formation and water affinity.[6] Additionally, mass-based measurements of chemical composition of aerosols are insensitive to the number of particles that have an important effect on cloud formation. The number of particles and their chemical components significantly affect cloud droplet number concentration, which is an important parameter to determine cloud properties such as cloud lifetime and reflectivity.[17] Thus, continuous measurements of the chemical composition and mixing state of size-resolved particles are important to better understand their roles in atmospheric chemistry, cloud formation, and the earth's radiation budget.

In this study, measurements of the hygroscopicity, volatility, and mixing state of size-selected submicrometer particles over the Arctic Ocean and the Pacific Ocean were conducted during an 11 937 km cruise (32 days) (9/7/2013−10/13/2013). It was reported that the sea ice area over the Arctic Ocean is minimal, and the delivery of nutrients from river (e.g., Mackenzie River) into the Arctic Ocean is intense in September.[18,19] The concentration of iron which has been known as a limiting nutrient for biological activity in the ocean was significantly affected by seasonal input of the discharge of rivers and seasonal ice-melting.[20,21] Thus, both the highest sea ice melting and the intense nutrient discharge from rivers to the Arctic Ocean in September will be useful to study the effect of the biological activity in the ocean on the aerosol properties.

Hygroscopic particles typically take up water, causing their size (or surface area) to increase, which enhances their light scattering potential (with subsequent effects on radiation balance), provides a greater available surface area for gas phase reactants,[22,23] and increases the effectiveness of cloud condensation nucleus (CCN) development.[24] The volatility measurement is useful to identify the existence of volatile organic species of the size-selected particles at a certain temperature.[25] The relative contributions of the "hygroscopic and non-volatile" nss-sulfate and sea salt species (with sea salt having a higher hygroscopic growth factor (HGF) than nss-sulfate) and the "less-hygroscopic and volatile" organic species to the size-resolved submicrometer particles can be determined by using both hygroscopicity and volatility data.[26] At the heater temperature of 100 °C, ammonium sulfate and other inorganic species (e.g., salts) are not volatile, while volatile organic species (e.g., *n*-alkane and dicarboxylic acid) are completely volatilized. Certain organics that were not volatilized at 100 °C can be considered as nonvolatile organics. The number size distribution of the submicrometer particles (30−600 nm) was measured with the differential mobility particle sizer (DMPS), and the total concentrations of particles larger than 2.5 and 10

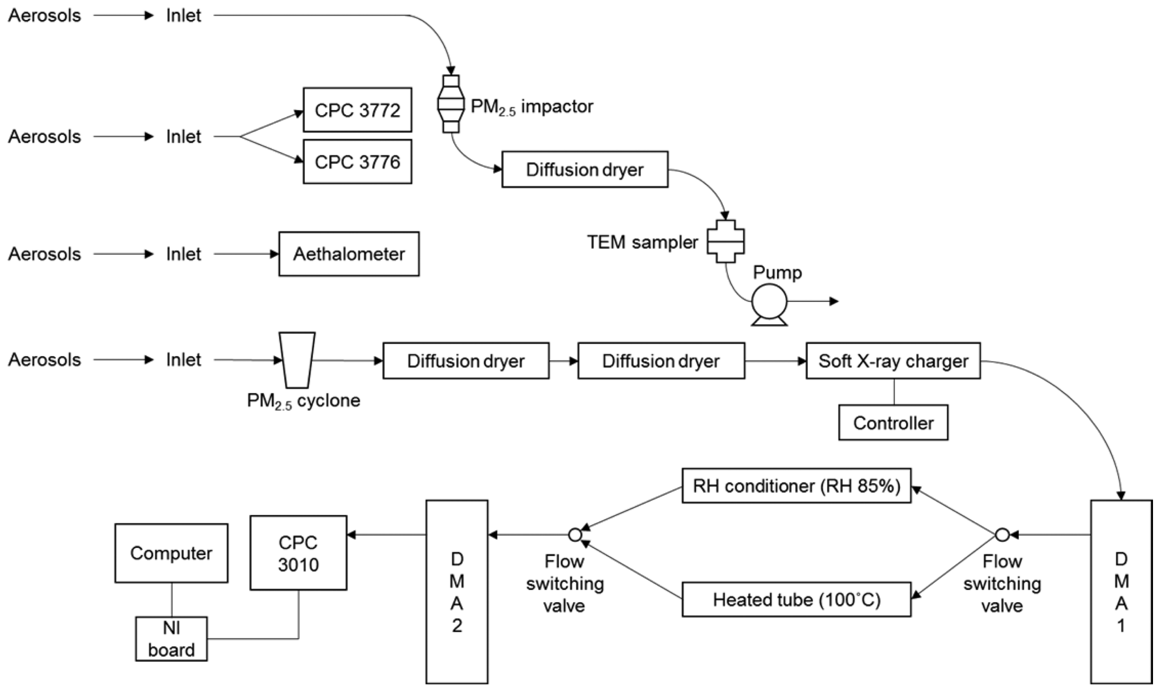

Figure 2. A schematic of aerosol sampling and measurement setup.

nm were measured with the two CPCs having different size cuts. The difference in the total number concentrations (i.e., number concentration of particles from 2.5 to 10 nm) from two CPCs can be used for examination of nanoparticle formation events during the cruise, leading to a better understanding of the nucleation process under the MBL.[27−29] Black carbon (BC) concentration, particle morphology and elemental composition, air mass back trajectory, and satellite data were also used to gain insight into aerosol formation and transport.

■ EXPERIMENTAL METHODS

Continuous measurements were conducted on board the ARAON ice breaker ship (Korea Polar Research Institute (KOPRI), Korea)[30] over the Arctic Ocean (departing from Barrow (USA), through the Beaufort Sea and Chukchi Sea, and arriving at Nome (USA); cruise 1, 5862 km) and the Pacific Ocean (departing from Nome (USA), through the Bering Sea, Sea of Okhotsk, and East Sea, and arriving at Gwangyang (Korea); cruise 2, 6075 km) as shown in Figure 1. In the first cruise, the ship departed from Barrow (USA) on 9/7/2013, traveled over the Beaufort Sea, performing 10 stops between the Mackenzie Trough and Tingmiark Valley in 10 days, and returned to Nome (USA) through the Chukchi Sea on 9/29/2013 as shown in Figure 1a. In the second cruise, the ship departed from Nome on 9/29/2013, traveled over the Bering Sea, Sea of Okhotsk, and East Sea and arrived at Gwangyang (Korea) on 10/13/2013, as shown in Figure 1b.

The aerosol sampling inlet was placed on the front deck of the ship (13 m above the sea level), far away from the ship exhaust (located 19 m above the sea level). After entering the inlet, aerosols passed through a stainless steel tube with an inner diameter of $^1/_4$ in. and a length of 1.2 m, and they were dried to approximately 7% relative humidity (RH) by a series of diffusion dryers before being introduced into aerosol instruments. The silica gels in the diffusion dryers were frequently replaced due to the high ambient RH (~90%) condition. The schematics of the sampling and aerosol instruments are shown in Figure 2.

For the determination of the hygroscopicity, volatility, and mixing state of size-selected submicrometer particles, the hygroscopicity and volatility tandem differential mobility analyzer (HVTDMA) technique[26,31−34] was used, which mainly consists of two DMAs, a humidifier, a heated tube, and a CPC (TSI 3010, USA). The size-selected particles from the first DMA were introduced into a humidifier (85% RH) or a heated tube (100 °C), and the resulting size change under the increased RH or temperature was measured with the second DMA and CPC. From this measurement, the hygroscopic growth factor (HGF), which is the ratio of the particle mobility diameter at an increased RH to that under the dry condition (10−15% RH), and the shrinkage factor (SF), which is the ratio of the particle mobility diameter at an increased temperature (100 °C) to that at room temperature (~25 °C), were obtained. At the heater temperature of 100 °C, ammonium sulfate and other inorganic species (e.g., salts) are not volatile, while the volatile organic species are completely volatilized. Note that the particles were dried before entering the HVTDMA system to remove any water in the particles. Occasionally, the heater temperature increased to 250 °C to remove the volatile species which was not volatilized at 100 °C and to identify the existence of nonvolatile species at 250 °C if they exist. For externally mixed particles, two or more different hygroscopic or volatile groups of particles can appear under increased RH or temperature, respectively, in the HVTDM data. For more details on the current HVTDMA system, refer to our previous studies.[26,32,35,36]

To measure the size distribution of submicrometer particles (30−600 nm), a differential mobility particle sizer (DMPS) consisting of a DMA and a CPC (TSI 3010, USA) was used. The lower detectable size of the DMA was 20−30 nm. An ultrafine CPC (UCPC) (TSI 3776, USA) and a CPC (TSI 3772, USA) were simultaneously used in tandem to determine total number concentrations of particles larger than the cut

Table 1. A Summary of Meteorology, Seawater Properties, and Aerosol Data during Cruises 1 and 2

	cruise 1	cruise 2
major locations	Arctic Ocean (Barrow, Beaufort Sea, Nome, and Chukchi Sea)	Pacific Ocean (Nome, Bering Sea, Sea of Okhotsk, East Sea, and Gwangyang)
date	9/7/2013−9/29/2013	9/29/2013−10/13/2013
average ambient temperature	−0.1 ± 1.1 °C	13.1 ± 3.1 °C
average RH	91 ± 5%	73 ± 9%
average wind speed	8.8 ± 2.0 m/s	12.9 ± 3.1 m/s
average wind direction	5.9 ± 23.4°	4.0 ± 23.6°
average seawater temperature	2.6 ± 1.0 °C	15.4 ± 3.5 °C
average chlorophyll-a concentration	3.4 ± 1.1 mg/m^3	1.0 ± 0.4 mg/m^3
average number concentration of particles larger than 10 nm	4,971 ± 5,987 #/cm^3 (CPC 3772)	3,648 ± 3,812 #/cm^3 (CPC 3772)
average number concentration of particles larger than 2.5 nm	11,910 ± 19,360 #/cm^3 (CPC 3776)	9,159 ± 17,780 #/cm^3 (CPC 3776)
average mean particle size	193 ± 72 nm	197 ± 24 nm
average black carbon concentration	20 ± 9 ng/m^3	502 ± 531 ng/m^3

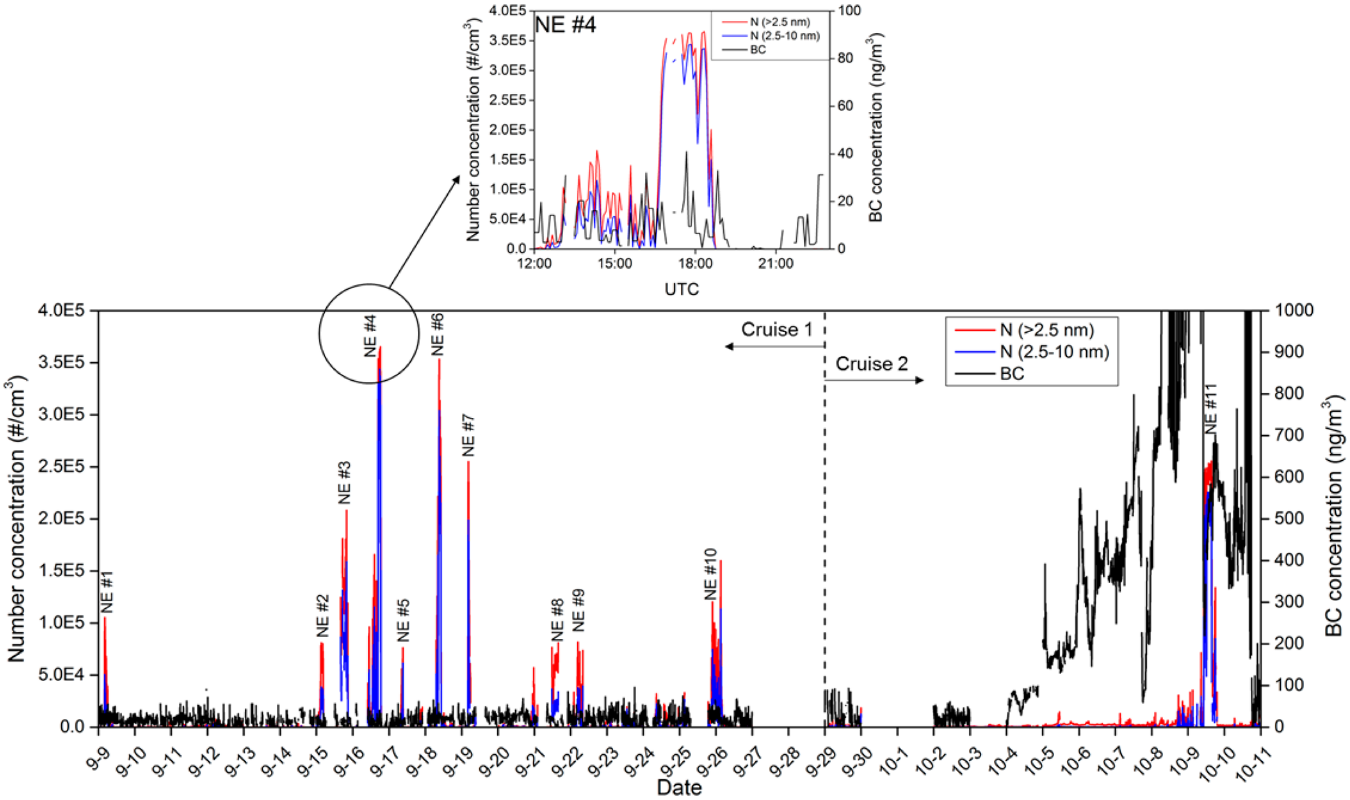

Figure 3. Time series of N(>2.5 nm) (particles/cm^3), N(2.5−10 nm) (particles/cm^3), and BC concentration (ng/m^3) during the entire sampling period. The NE represents nucleation event.

sizes of two CPCs. Both CPCs sampled the same ambient air through a common inlet. The TSI 3776 CPC has a cut size of 10 nm (i.e., it measures number concentration of particles larger than 10 nm), while the TSI 3772 UCPC has a cut size of 2.5 nm (i.e., the TSI model 3772 measures number concentration of particles larger than 2.5 nm). Detailed parameters of two CPCs are included in Table S1 in the Supporting Information. They have the same inlet with identical tube length and diameter, suggesting that transport and inlet losses will not be significantly different between two CPCs. Penetration of 6 nm particles into both CPC was calculated as included in Table S1 (Supporting Information). Difference in the two sets of CPC data were used to represent the number concentration of nanoparticles from 2.5 to 10 nm. This size bin can often be used to represent the nucleation mode particles (i.e., freshly nucleated particles). The size cuts in both CPCs which are not completely sharp, and different time responses of both CPCs can contribute to uncertainty in the calculation of the total particle number concentration. The average uncertainty can be calculated by using the CPC flow rate, coincidence correction, counting efficiency, and sampling efficiency giving ±10% for the determination of the total number concentration.[37] It is reported that the assignment of the difference in particle number concentrations between two CPCs to particles in the size range between two size cuts was reliable, based on the laboratory tests.[38]

The BC concentration was measured with an Aethalometer (AE22, Magee Scientific Co., USA). To determine the

Table 2. A Summary of Particle Number Concentration, BC Concentration, and Seawater Temperature (T) during Nucleation Events

date	time	air mass type	N(>2.5 nm) (#/cm^3)	N(2.5−10 nm) (#/cm^3)	N(2.5−10 nm)/N(>2.5 nm) (%)	BC (ng/m^3)	Seawater T (°C)
9/9/2013	04:00−06:30	Marine (Beaufort sea)	45,359 ± 12,881	16,390 ± 6,563	32 ± 5	22 ± 7	2.4 ± 0.1
9/15/2013	01:25−04:40	Marine (remote Arctic Ocean)	39,842 ± 13,696	16,172 ± 6,446	39 ± 4	8 ± 3	3.2 ± 0.1
9/15/2013	16:05−21:00	Marine (remote Arctic Ocean)	114,357 ± 25,694	68,993 ± 19,168	56 ± 7	11 ± 5	3.3 ± 0.2
9/16/2013	09:55−18:40	Marine (remote Arctic Ocean)	101,457 ± 58,995	77,481 ± 54,829	52 ± 12	12 ± 5	2.5 ± 0.2
9/17/2013	07:40−09:25	Marine (remote Arctic Ocean)	31,188 ± 10,431	13,567 ± 7,479	40 ± 10	8 ± 4	2.4 ± 0.1
9/18/2013	07:35−10:50	Marine (Beaufort sea)	161,795 ± 58,771	124,705 ± 50,275	66 ± 9	22 ± 5	0.4 ± 0.2
9/19/2013	04:05−06:30	Marine (Beaufort sea)	108,572 ± 36,289	61,922 ± 31,699	46 ± 11	16 ± 5	2.0 ± 0.1
9/21/2013	11:35−15:55	Marine (Beaufort sea)	53,383 ± 7,654	16,885 ± 3,802	30 ± 3	10 ± 4	0.9 ± 0.1
9/22/2013	04:10−08:05	Marine (Beaufort sea)	25,650 ± 12,063	10,876 ± 5,928	41 ± 9	26 ± 5	0.8 ± 0.1
9/25/2013−9/26/2013	20:55−04:45	Marine (remote Arctic Ocean)	48,462 ± 15,588	23,896 ± 10,178	45 ± 8%	26 ± 7	0.3 ± 0.1
10/9/2013	08:05−19:10	Continental (China and Japan)	161,296 ± 45,567	129,738 ± 45,708	66 ± 13	538 ± 52	21.3 ± 0.6

morphology and elemental composition of the particles, they were occasionally collected on a grid and analyzed by TEM (200 kV accelerating voltage and 100 μA beam current) (JEOL JEM-2100F, Japan) and energy dispersive spectroscopy (EDS) (OXFORD INCAx-sight, Japan). The number concentrations from two CPCs, BC concentration from the Aethalometer, and meteorological and GPS data were obtained for 24 h every day. Hygroscopicity and volatility measurement was performed from 08:00 to 22:00 every day during cruise. TEM sampling time and duration are summarized in Table S3 in Supporting Information.

The air mass back trajectory (72 h) data arriving at elevations of 15 and 500 m above the ground level were obtained by using the Hybrid Single-Particle Lagrangian Integrated Trajectory (HYSPLIT version 4 model) (available at http://ready.arl.noaa.gov/) for the investigation of air mass transport during the cruise. Satellite data (Aqua MODIS) (http://oceancolor.gsfc.nasa.gov) were obtained to infer the chlorophyll-a concentration (a possible indicator of biological activity over the ocean). Meteorological (wind speed, wind direction, T, and RH) and GPS (latitude, longitude, and ship speed) data were obtained from an air weather system (AWS) installed in the ship.

Data suspected of being resultant from the ship exhaust emission were excluded from further analysis. To remove data affected by the ship emission, BC, wind, and number concentration data were used. A sudden increase (e.g., spike) in BC or number concentration, or wind data with a certain wind direction (160°−200°) originating directly from the ship exhaust was used to exclude data possibly affected by the ship exhaust emission. Typically, the nucleation events discussed later were clearly distinguishable from the ship exhaust emission because the enhanced number concentration during the nucleation events lasted for multiple hours with a low BC concentration.

RESULTS AND DISCUSSION

The ship voyage was classified into two major cruises. During cruise 1, the ship traveled around the Arctic Ocean (Barrow, Beaufort Sea, Nome, and Chukchi Sea), while during cruise 2, the ship traveled through the Bering Sea, Sea of Okhotsk, and East Sea, arriving at Gwangyang (Korea). This area (cruise 1) was considered a highly biologically active area based on satellite data (chlorophyll-a concentration), as included in Figure 1a compared to cruise 2. The particulate organic carbon concentration in the seawater was also high in this area (satellite data not shown). During the second cruise, the satellite-derived chlorophyll-a concentration over the ship route was much lower than that during the first cruise, as shown in Figure 1b. The temperature was higher, and the RH was lower and more variable during cruise 2 than during cruise 1. A summary of sampling days, major locations, meteorological data, and seawater properties during cruises 1 and 2 is included in Table 1.

The time series of the particle number concentrations (N(>2.5 nm) and N(2.5−10 nm)) and the BC concentration during the sampling period are shown in Figure 3. N(2.5−10 nm) was obtained from the difference between the two CPC data sets. On the basis of the air mass trajectory, the aerosol data under marine and continental influence were also determined. During cruise 1, the average total number concentration of particles (N(>2.5 nm)) under marine influence was found to be 14 440 particles/cm^3, which is much higher than the values observed in the remote oceans in previous studies.[39,40] This was caused by multiple nucleation events (significant increases of particles in the size range of 2.5 to 10 nm) under marine influence occurred during cruise 1 (see Figure 3 and Table 2). When data during the nucleation events were excluded, the total number concentration under marine influence decreased to 1048 particles/cm^3, which is similar to the value reported in the tropical Atlantic Ocean,[41] and higher than ones reported in the remote background oceans.[42−45] The minimum detectable size varied among studies, leading to the

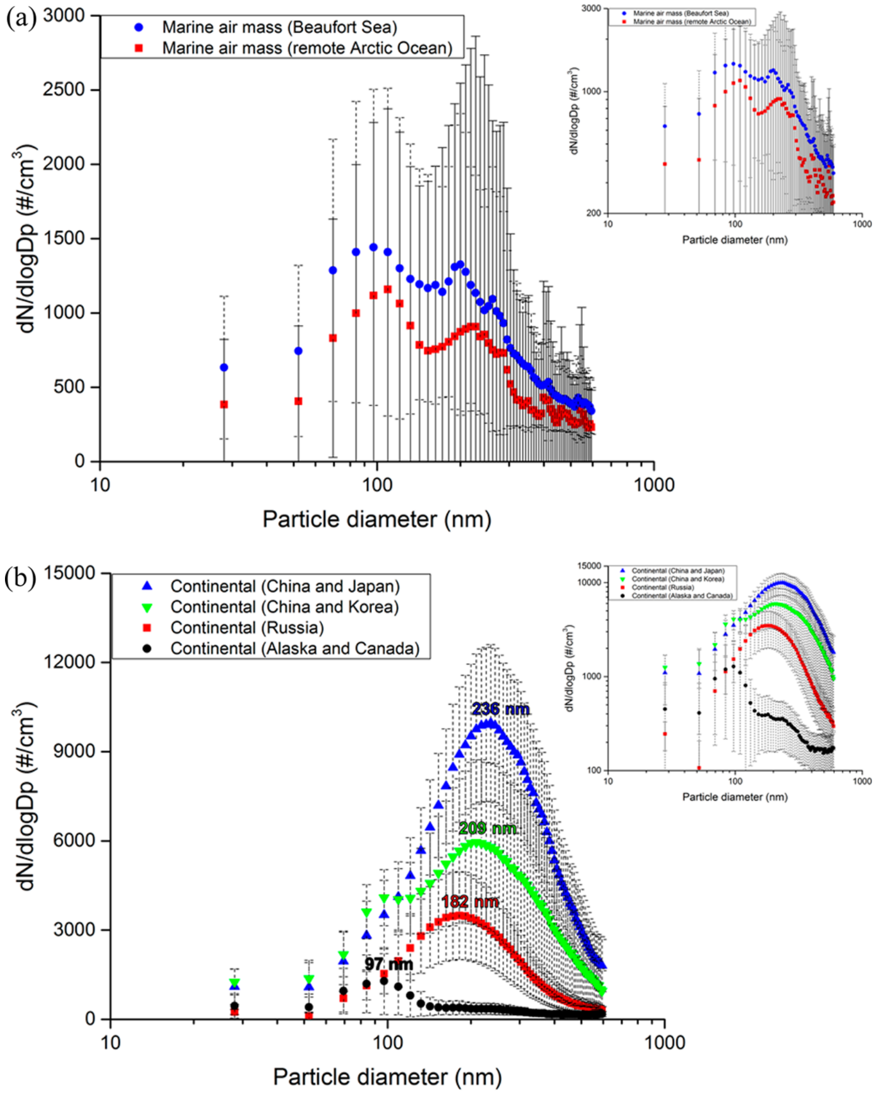

Figure 4. Number size distributions (30−600 nm) in (a) marine air masses originating from the remote Arctic Ocean and Beaufort Sea and (b) continental air masses originating from Alaska and Canada, Russia, China, and Japan, and China and Korea. Subsets with log-scale *y*-axis are added. The error bar indicates the standard deviation.

difference in the total number concentration especially when the nucleation event often occurred. Note that the minimum particle size for the determination of the total number concentration goes down to 2.5 nm in our measurement. It has been reported that nucleation often happened in coastal areas,[46−49] while few nucleation events were observed in the remote marine environment.[50] In our measurements, multiple nucleation events occurred during cruise 1. The closest distance to the coast was 60 km during the cruise 1, and this coastal area has few significant anthropogenic sources. The BC concentration was also very low (20 ng/m^3 on average) during the entire cruise 1, as shown in Figure 3, suggesting that the effect of local anthropogenic sources on the production of aerosols should be small.

The chlorophyll-a is the primary molecule responsible for photosynthesis and can be found in every single photosynthesizing organism (e.g., land plant, algae, and cyanobacteria).[51,52] Since all phytoplankton (the foundation of marine food chain) have chlorophyll-a, the chlorophyll-a can be used as simple proxy for phytoplankton biomass in the ocean.[53,54] In this study, the chlorophyll-a concentration was used as an indicator for biological activity in the ocean. As shown in Figure 1, the chlorophyll-a concentration during cruise 1 was much higher than that during cruise 2. The abundant organic matter resulting from the strong biological activity in the ocean can contribute to the production of primary biological particles and the release of biological organic compounds. The biological organic compounds can be involved in new particle formation and particle growth. This is important because those particles will have a strong potential for CCN production over the ocean. Previous studies reported that the nucleation and growth of particles by iodine compounds and sulfuric acid in remote marine areas is possible, but only a small fraction can grow to larger particles.[7] The possibility of the entrainment of aerosols nucleated in the free troposphere to the MBL cannot be ruled out. The possible nucleation and growth mechanism will be discussed in later sections with hygroscopicity and volatility results. During cruise 2, a frequent continental influence was observed. The average BC concentration and total particle number concentration (N(>2.5 nm)) under continental influence were 387 ng/m^3 and 7,638 particles/cm^3, respectively. Only one nucleation event was observed during cruise 2. The

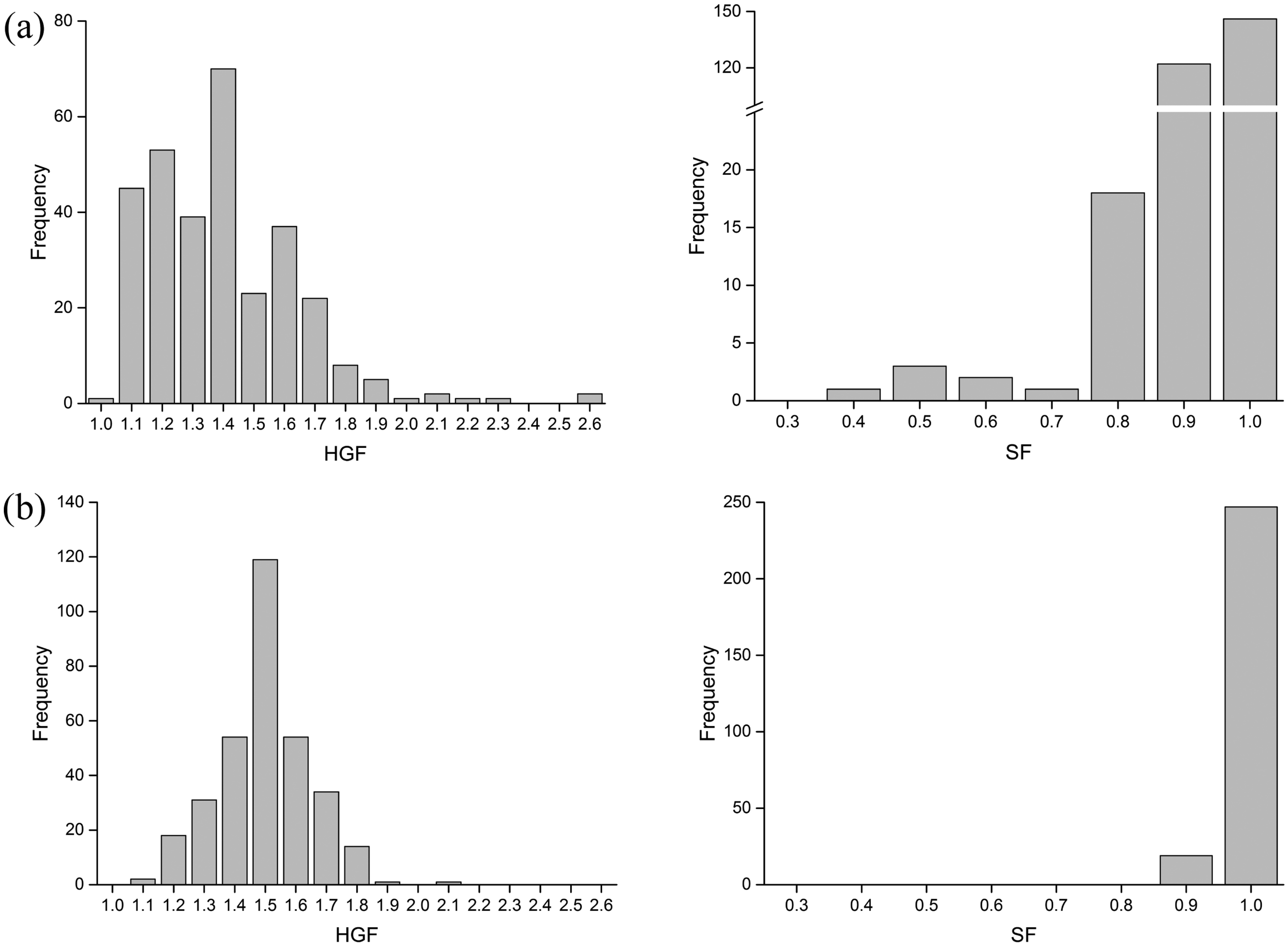

Figure 5. Distributions of HGF and SF of the size-selected submicrometer particles (50−220 nm) during (a) cruise 1 and (b) cruise 2.

BC concentration significantly increased under the continental influence during cruise 2, as shown in Figure 3.

The average number size distributions of particles (30 nm−600 nm) under marine and continental influences with varying air mass types are shown in Figure 4. Although the size distributions of particles smaller than 30 nm were not available with the current experimental setup, a clear difference was observed among varying air masses. Multiple modes (100−110 nm, 200−230 nm, 270−300 nm, and 400−420 nm) were observed for particle size distributions under marine influence, as shown in Figure 4a (the nucleation mode less than 30 nm would not be detected here due to the size limitation of the instrument used, but the number concentration of particles from 2.5 to 10 nm was determined as discussed in the previous section). The multiple mode of the size distribution suggests that the different types of particles exist because of their varying sources and formation mechanisms (primary and secondary). Usually, one mode in the size distribution appeared for particles produced from single source or formation mechanism. On the other hand, a single dominant peak in the size distribution became evident upon interaction with the continental air mass. The number concentration (30 nm−600 nm) of aerosols was much lower than that of the aerosols influenced by the continental air masses, and the highest concentration was observed for air masses from China passing over Japan. The mean particle size in the single dominant mode of particles under continental influence increased from 100 nm (Alaska and Canada) to 180 nm (Russia), 210 nm (China and Korea), and 240 nm (China and Japan) as the air mass originated from more polluted continental areas.

Hygroscopicity, Volatility, and Mixing State. As discussed in the previous section, more frequent nucleation events and multiple modes in the particle size distribution were observed during cruise 1, where the marine influence was prevalent. Hygroscopicity and volatility data could provide more useful insight into the particle production mechanism. It has been reported that the ocean biological activity greatly affected the *ratios* of organics to nss-sulfate and sea salts in the submicrometer particles in the remote ocean.[10,55] The HGFs at 90% RH for ammonium sulfate, ammonium bisulfate, sea salts, water-soluble organic matter (WSOM), and water insoluble organic matter (WIOM) were assigned as 1.7, 1.8, 2.0, 1.2, and 1.0, respectively.[55] Our laboratory experiments using various aerosols with the current HVTDMA system had similar results to the above.[32] At the heater temperature of 100 °C, ammonium sulfate and other inorganic species (e.g., salts) are not volatile, while only volatile organic species are completely volatilized. Nonvolatile organics were defined when they were not volatilized at 100 °C. Thus, the nss-sulfate and sea salt species (with the sea salt having a higher HGF than the sulfate) were "hygroscopic and non-volatile", and the volatile organic species were "less hygroscopic and volatile", as determined by simultaneously measuring the hygroscopicity and volatility of the size-selected particles.

The distributions of the HGF and SF of the size-selected submicrometer particles (50 nm-220 nm) during cruises 1 and 2 are compared in Figure 5 panels a and b, respectively. As shown in Figure 5a, much wider ranges of HGF and SF were observed during cruise 1 compared to cruise 2. Additionally, multiple peaks of HGF were found in 1.1−1.2, 1.4, and 1.6, and a significant amount of the volatile species existed in the particles (i.e., the low SF) during cruise 1. The HGF values of 1.4 and 1.6 are consistent with sulfates with varying amounts of organic components. The low HGF mode is mainly attributable to biological organic components (less hygroscopic). Note that during cruise 1, the ship passed over the biologically active ocean, suggesting that biological organic materials (both primary and secondary) should be abundant (i.e., the low HGF would be linked with the oceanic biological activity). Prather et al. (2013) showed that the HGF of the SSA produced from natural seawater in their continuous wave breaking chamber significantly decreased with increasing concentrations of biological materials in the seawater.[6] The abundant organic matters resulting from the strong biological activity in the ocean might contribute to the releases of both biological particles (primary aerosols) and volatile organic species over the ocean. The volatile organic compounds can be involved in the new particle formation and particle growth (secondary aerosols) as discussed in the previous section. Since data for precursor vapors and composition of nanoparticles (<10 nm) were not available, the major precursor gases responsible for nucleation were not certain. However, the indirect chemical composition of submicrometer particles based on hygroscopicity and volatility, and results for the relation of chlorophyll-a concentration to the nanoparticle production suggest that biological organic compounds could play a certain role in formation and growth of nanoparticles. It has been suggested that sulfur, isoprene, and iodine species could be produced by marine biota, and that such biogenic species could be involved in the new particle formation and growth.[47,56−59]

On the other hand, during cruise 2 (in which the continental influence was prevalent), a single peak of HGF (1.5) was found (falling into a single dominant mode), and the amount of volatile *organic* species was relatively small. The HGF and SF data are consistent with our hypothesis that volatile organic species significantly contributed to the submicrometer aerosols under marine influence (i.e., they participated in the formation and growth of particles, leading to multiple modes of the size distribution). The fraction of submicrometer particles having an external mixing state (i.e., each particle of the same size has different compositions) was small (the external mixture exists in 2% of the total measurements). Most of them were internally mixed. This suggests that highly hygroscopic (sea-salt) particles do not exist solely in the submicrometer particles and that the internal mixtures of nss-sulfates, volatile/semivolatile organics, and sea salts in varying fractions should be the dominant type of submicrometer particles (as will be discussed in the following section). No significant dependence of HGF and SF on particle size was observed (see Figure S1 in Supporting Information) in the range of 50 to 220 nm, suggesting that the compositional change with size in this range should not be large.

The measured HGF and volume fraction of the volatile species were compared with data estimated from mixtures of specific chemical species of known hygroscopicity and volatility by using the Zdanovskii−Stokes−Robinson (ZSR) relationship,[60] as shown in Figure 6. The ZSR method assumes that each species independently takes up water at the given RH. The mixing components for the submicrometer particles are assumed to be hygroscopic and nonvolatile sea salt (HGF = 2.0 and SF = 1.0), hygroscopic and nonvolatile nss-sulfate (HGF = 1.7 and SF = 1.0), volatile and nonhygroscopic organics (HGF = 1.0 and SF = 0.0), and nonvolatile and hygroscopic organics (HGF = 1.2 and SF = 1.0) as summarized in Table S2 in the Supporting Information. Dust components (nonhygroscopic and nonvolatile) were excluded because the amount of dust particles would be small in the submicrometer particles tested here. The estimated HGF as a function of the volume fraction of volatile species for internal mixtures of two or three components is plotted in Figure 6. As shown in Figure 6a, the submicrometer particles from cruise 1 can be various internal mixtures (data scattered over three mixture curves: a mixture of volatile and nonhygroscopic organic species (HGF = 1.0) and nonvolatile and less-hygroscopic organic species (HGF = 1.2); a mixture of volatile and nonhygroscopic organic species (HGF = 1.0), nonvolatile and less-hygroscopic organic

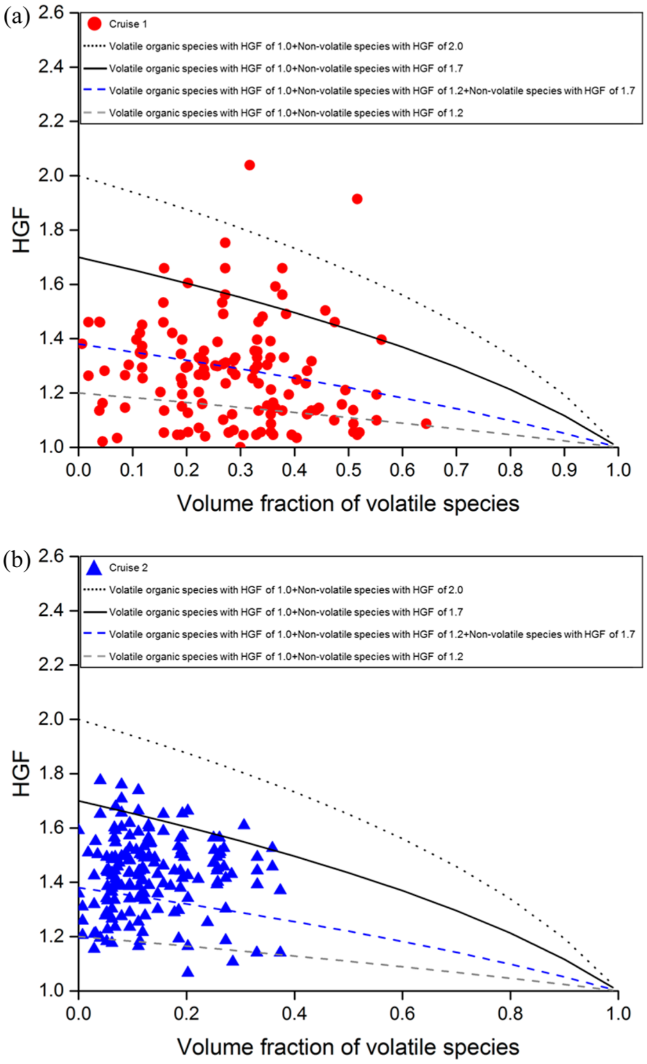

Figure 6. Measured HGF as a function of the volume fraction of volatile species and the estimated HGF curves for multicomponent mixtures using the Zdanovskii−Stokes−Robinson (ZSR) relationship during (a) cruise 1 and (b) cruise 2.

species (HGF = 1.2), and nonvolatile and hygroscopic nss-sulfate (HGF = 1.7); and a mixture of volatile and nonhygroscopic organic species (HGF = 1.0) and nonvolatile and hygroscopic nss-sulfate (HGF = 1.7), with varying volume fractions of volatile species). The mixture of volatile and nonhygroscopic organic species (HGF = 1.0) and nonvolatile and hygroscopic sea salt (HGF = 2.0) rarely exists in the submicrometer particles. During cruise 2, the distribution of the submicrometer particles were more concentrated between two mixture curves (a mixture of volatile and nonhygroscopic organic species (HGF = 1.0), nonvolatile and less hygroscopic organic species (HGF = 1.2), and nonvolatile and hygroscopic nss-sulfate (HGF = 1.7) and a mixture of volatile and nonhygroscopic organic species (HGF = 1.0) and nonvolatile and hygroscopic nss-sulfate (HGF = 1.7)), with a smaller amount of the volatile species compared to that from cruise 1. The higher amount of nonvolatile and hygroscopic nss-sulfate should be included in the mixture to explain the measured HGF and SF.

The change in particle size (i.e., volume fraction of the volatile species) as a function of the heater temperature (20 °C to 250 °C) on 9/11/2013 (cruise 1) and 10/10/2013 (cruise 2) is shown in Figure 7. The 110 nm particles were selected because the peak sizes in the number size distribution data on both days were close to the 110 nm. On 9/11/2013 (cruise 1), the volatile organic species first started to evaporate below 100 °C, and then the nss-sulfates and less volatile organic species evaporated above 100 °C until almost complete evaporation occurred at 250 °C. This is consistent with the existence of a higher amount of volatile species during cruise 1, as discussed in the previous section. On 10/10/2013 (cruise 2), little volatile organic species that could evaporate below 100 °C existed, and nss-sulfate started to evaporate at 150 °C, which is consistent with the existence of a significant amount of nss-sulfate during cruise 2. The nss-sulfate can originate from both anthropogenic sources (anthropogenic SO_2 conversion) and biogenic marine sources (i.e., the dimethyl-sulfide (DMS) oxidation conversion).[61,62] Additionally, a significant amount of material was not completely evaporated at 250 °C, suggesting that those particles contain nonvolatile species such as minerals or biological materials.

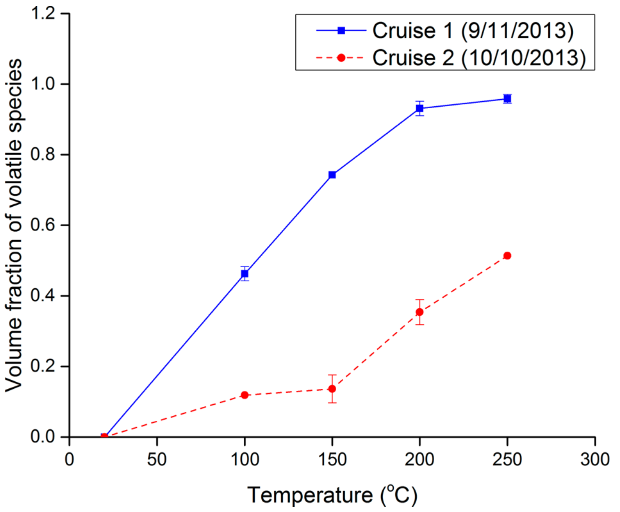

Figure 7. Volume fraction of volatile species of 110 nm particles as a function of the heater temperature (20 °C to 250 °C) on 9/11/2013 (cruise 1) and 10/10/2013 (cruise 2).

The effect of the air mass on aerosol properties was examined. The major air mass types during the cruise are summarized in Table 3 (air mass trajectory data arriving at elevations of 15 and 500 m above the ground level are shown in Figure S2 in the Supporting Information). The air mass was classified into marine and continental air masses based on air mass back trajectory analysis. When the air mass (arriving at elevations of 15 and 500 m above the ground level) originated from ocean and had no contact with land during at least 72 h, the air mass was classified as marine air mass.[63−65] During cruise 1, the marine air masses originating from the remote Arctic Ocean and Beaufort Sea were dominant, while continental air masses originating from Russia, Japan, Korea, and China became abundant during the cruise 2. A summary of the aerosol properties with varying air masses is included in Table 3. As shown, when the ship approached land and/or had influence from continental air masses, enhancement of the BC concentration was often observed (the BC concentration was the highest when the air mass came from China and Japan), suggesting that the BC concentration can be used as an indicator of continental/anthropogenic source influence. But, the BC was not the only indicator for the continental source influence (e.g., the nss-sulfate can also be produced from anthropogenic activity).[15] The particle number concentration should not be considered as the indicator for anthropogenic source influence because the number concentration was much

Table 3. A summary of Aerosol Properties *with* Varying Air Mass Types

air mass type	date	HGF	volume fraction of volatile species (%)	*N* (>2.5 nm) (#/cm^3)	*N* (2.5−10 nm) (#/cm^3)	BC (ng/m^3)
marine air mass (remote Arctic Ocean):	9/15, 9/16, 9/17, 9/25, 9/26, 9/28, 9/29	1.40 ± 0.14	24 ± 7	22 670 ± 28 920	14 820 ± 23 660	17 ± 9
marine air mass (Beaufort Sea):	9/8, 9/9, 9/10, 9/13, 9/18, 9/19, 9/20, 9/21, 9/27	1.32 ± 0.18	27 ± 6	10 390 ± 19 400	6 870 ± 15 600	18 ± 6
continental air mass (Alaska and Canada)	9/11, 9/12, 9/14	1.31 ± 0.08	30 ± 9	777 ± 538	241 ± 282	16 ± 7
continental air mass (Russia)	10/2−10/6	1.41 ± 0.07	7 ± 1	1545 ± 705	190 ± 103	167 ± 73
continental air mass (China and Japan)	10/8−10/10	1.46 ± 0.07	9 ± 2	24 970 ± 31 150	16 530 ± 25 980	947 ± 849
continental air mass (China and Korea)	10/11−10/12	1.52 ± 0.06	15 ± 4	4310 ± 2744	595 ± 840	593 ± 360
average during the whole sampling period	9/7/2013−10/13/2013	1.39 ± 0.09	19 ± 6	9772 ± 18 300	5976 ± 14 860	188 ± 335

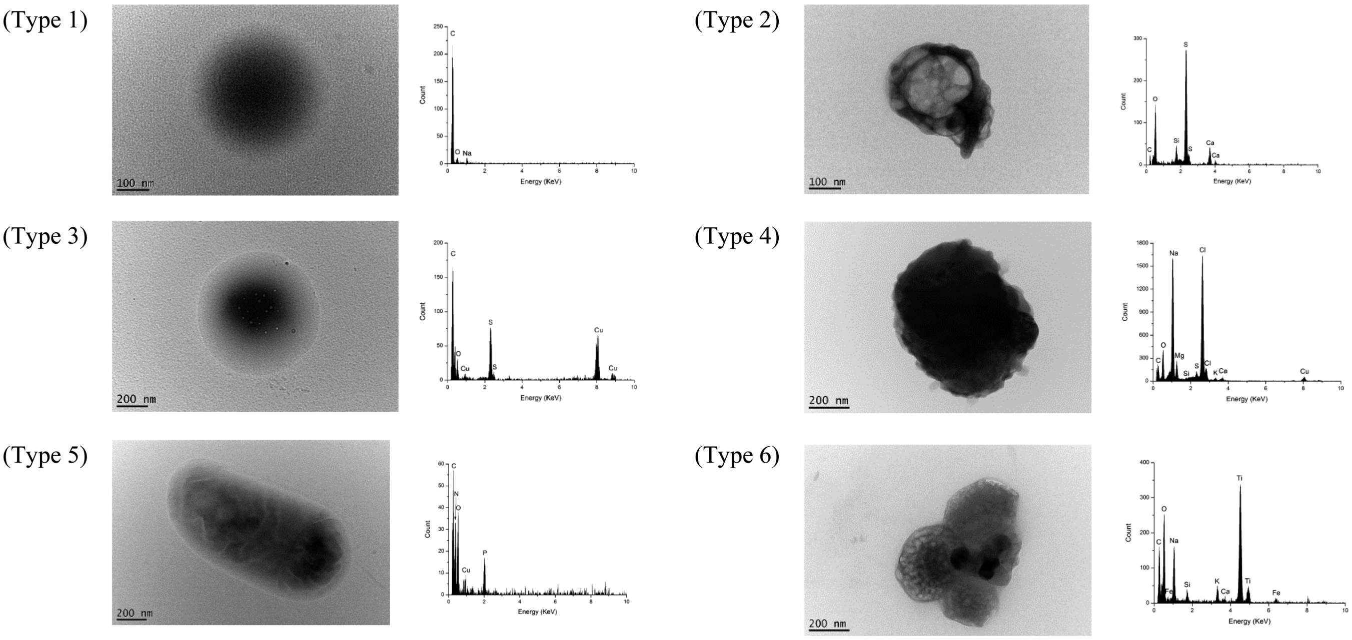

Figure 8. TEM/EDS data for C-rich mixture (type 1), S-rich mixture (type 2), C/S-rich mixture (type 3), Na-rich mixture (type 4), C/P-rich mixture (type 5), and mineral-rich mixture (type 6). The major elements of the type 6 particles differed depending on the type of minerals included.

higher under marine influence in this study due to the frequent nucleation events compared to under continental influence.

Elemental and Morphological Properties. The elemental composition and morphology of the particles were analyzed using the TEM/EDS data. TEM sampling time and duration were summarized in Table S3 in the Supporting Information. Note that some volatile particles could not be detected by the TEM because of their possible evaporation under the low vacuum conditions. Additionally, note that the number of particles analyzed (257 particles) would not be sufficient to draw solid conclusions. However, the morphological and elemental data can still provide useful insights into the particle types observed during the cruise. Also, identification of biological particles can provide supporting evidence for the degree of biological activity in the ocean. The major types of submicrometer particles were categorized as C-rich mixture (type 1), S-rich mixture (type 2), C/S-rich mixture (type 3), Na-rich mixture (type 4), C/P-rich mixture (type 5), and mineral-rich mixture (type 6) as shown in Figure 8. The Na-rich mixture (type 4), C/P-rich mixture (type 5), and mineral-rich mixture (type 6) were also abundant at the upper end of the submicrometer range or larger than 1 μm. Type 1 represents carbonaceous particles (i.e., C-rich particles). Because volatile carbonaceous particles are difficult to detect due to their rapid evaporation in the low vacuum in the TEM, the actual number fraction of type 1 particles should be higher than the measured value. Type 2 represents nss-sulfate particles, where a dominant peak of S exists without sea salt species (e.g., Na, Cl, and Mg). These particles would be produced by the oxidation of the DMS or transported from continental sources. In type 3 particles, both C and S peaks are dominant (i.e., organics and sulfates would be internally mixed). For type 4 particles, the typical elements of sea salts (Na, Cl, Mg, Ca, and S) were detected. Type 5 may represent refractory biological particles, which always contain P. Type 6 particles include various crustal elements. Interestingly, type 5 (P-containing) particles were observed more often during cruise 1, suggesting that the ship traveled within a strongly biologically active area during this cruise.

The chlorophyll-a concentration used to indicate biological activity in the ocean, hygroscopicity, and volatility data used to find the biological volatile organic compounds (secondary) in the submicrometer particles, and morphological and elemental composition used to find the biological particles (primary), all support that the biological activity in the ocean significantly affected properties of submicrometer particles over the ocean

■ ASSOCIATED CONTENT

Ⓢ Supporting Information

The Supporting Information is available free of charge on the ACS Publications website at DOI: 10.1021/acs.est.5b01505.

> Table S1, operating parameters of two CPCs and transport loss calculation; Table S2, type of mixtures with mixing components; Table S3, sampling date and time for TEM/EDS sampling. Figure S1, HGF and volume fraction of volatile species as a function of particle size; Figure S2, air mass trajectory during cruises (pdf)

■ AUTHOR INFORMATION

Corresponding Authors

*Phone: 82-32-760-5305; fax: 82-32-760-5399; e-mail: yjyoon@kopri.re.kr.
*Phone: 82-62-715-3279; fax: 82-62-715-2434; e-mail: kpark@gist.ac.kr.

Notes

The authors declare no competing financial interest.

■ ACKNOWLEDGMENTS

The research was supported by the National Leading Research Laboratory Program (NRF-2011-0015548) of the Ministry of Science, ICT, and Future Planning (MSIP) and the National Research Foundation (NRF) of Korea. This work was also funded by a National Research Foundation of Korea Grant funded by the Korean Government (NRF-2011-0021064 and NRF-2014M3C8A5028593).

REFERENCES

(1) Houghton, J. T.; Ding, Y.; Griggs, D. J.; Noguer, M.; van der Linden, P. J.; Xiaosu, D.*Climate Change 2001: The Scientific Basis* Contribution of Working Group I to the Third Assessment Report of the Intergovernmental Panel on Climate Change (IPCC) Cambridge University Press: 2001

(2) Andreae, M. O. Climatic effects of changing atmospheric aerosol levels. *World Survey of Climatology* **1995**, *16*, 347−398.

(3) Andreae, M. O.; Rosenfeld, D. Aerosol-cloud-precipitation interactions. Part 1. The nature and sources of cloud-active aerosols. *Earth-Sci. Rev.* **2008**, *89* (1−2), 13−41.

(4) Gantt, B.; Xu, J.; Meskhidze, N.; Zhang, Y.; Nenes, A.; Ghan, S. J.; Liu, X.; Easter, R.; Zaveri, R. Global distribution and climate forcing of marine organic aerosol-Part 2: Effects on cloud properties and radiative forcing. *Atmos. Chem. Phys.* **2012**, *12* (14), 6555−6563.

(5) Bellouin, N.; Boucher, O.; Haywood, J.; Reddy, M. S. Global estimate of aerosol direct radiative forcing from satellite measurements. *Nature* **2005**, *438* (7071), 1138−1141.

(6) Prather, K. A.; Bertram, T. H.; Grassian, V. H.; Deane, G. B.; Stokes, M. D.; DeMott, P. J.; Aluwihare, L. I.; Palenik, B. P.; Azam, F.; Seinfeld, J. H.; Moffet, R. C.; Molina, M. J.; Cappa, C. D.; Geiger, F. M.; Roberts, G. C.; Russell, L. M.; Ault, A. P.; Baltrusaitis, J.; Collins, D. B.; Corrigan, C. E.; Cuadra-Rodriguez, L. A.; Ebben, C. J.; Forestieri, S. D.; Guasco, T. L.; Hersey, S. P.; Kim, M. J.; Lambert, W. F.; Modini, R. L.; Mui, W.; Pedler, B. E.; Ruppel, M. J.; Ryder, O. S.; Schoepp, N. G.; Sullivan, R. C.; Zhao, D. Bringing the ocean into the laboratory to probe the chemical complexity of sea spray aerosol. *Proc. Natl. Acad. Sci. U. S. A.* **2013**, *110* (19), 7550−7555.

(7) Vuollekoski, H.; Kerminen, V. M.; Anttila, T.; Sihto, S. L.; Vana, M.; Ehn, M.; Korhonen, H.; McFiggans, G.; O'Dowd, C. D.; Kulmala, M. Iodine dioxide nucleation simulations in coastal and remote marine environments. *J. Geophys. Res.* **2009**, *114* (2), D02206.

(8) Cavalli, F.; Facchini, M. C.; Decesari, S.; Mircea, M.; Emblico, L.; Fuzzi, S.; Ceburnis, D.; Yoon, Y. J.; O'Dowd, C. D.; Putaud, J. P.; Dell'Acqua, A. Advances in characterization of size-resolved organic matter in marine aerosol over the North Atlantic. *J. Geophys. Res.* **2004**, *109* (24), 1−14.

(9) Andreae, M. O. Aerosols before pollution. *Science* **2007**, *315* (5808), 50−51.

(10) O'Dowd, C. D.; Facchini, M. C.; Cavalli, F.; Ceburnis, D.; Mircea, M.; Decesari, S.; Fuzzi, S.; Young, J. Y.; Putaud, J. P. Biogenically driven organic contribution to marine aerosol. *Nature* **2004**, *431* (7009), 676−680.

(11) Lohmann, U.; Leck, C. Importance of submicron surface-active organic aerosols for pristine Arctic clouds. *Tellus, Ser. B* **2005**, *57* (3), 261−268.

(12) Lohmann, R.; Jaward, F. M.; Durham, L.; Barber, J. L.; Ockenden, W.; Jones, K. C.; Bruhn, R.; Lakaschus, S.; Dachs, J.; Booij, K. Potential contamination of shipboard air samples by diffusive emissions of PCBs and other organic pollutants: Implications and solutions. *Environ. Sci. Technol.* **2004**, *38* (14), 3965−3970.

(13) Phinney, L.; Richard Leaitch, W.; Lohmann, U.; Boudries, H.; Worsnop, D. R.; Jayne, J. T.; Toom-Sauntry, D.; Wadleigh, M.; Sharma, S.; Shantz, N. Characterization of the aerosol over the sub-arctic north east Pacific Ocean. *Deep Sea Res., Part II* **2006**, *53* (20−22), 2410−2433.

(14) Ceburnis, D.; Garbaras, A.; Szidat, S.; Rinaldi, M.; Fahrni, S.; Perron, N.; Wacker, L.; Leinert, S.; Remeikis, V.; Facchini, M. C.; Prevot, A. S. H.; Jennings, S. G.; Ramonet, M.; O'Dowd, C. D. Quantification of the carbonaceous matter origin in submicron marine aerosol by 13C and 14C isotope analysis. *Atmos. Chem. Phys.* **2011**, *11* (16), 8593−8606.

(15) Shank, L. M.; Howell, S.; Clarke, A. D.; Freitag, S.; Brekhovskikh, V.; Kapustin, V.; McNaughton, C.; Campos, T.; Wood, R. Organic matter and non-refractory aerosol over the remote Southeast Pacific: Oceanic and combustion sources. *Atmos. Chem. Phys.* **2012**, *12* (1), 557−576.

(16) Frossard, A. A.; Russell, L. M.; Burrows, S. M.; Elliott, S. M.; Bates, T. S.; Quinn, P. K. Sources and composition of submicron organic mass in marine aerosol particles. *J. Geophys. Res. D: Atmos.* **2014**, *119* (22), 12977−13003.

(17) Nenes, A.; Charlson, R. J.; Facchini, M. C.; Kulmala, M.; Laaksonen, A.; Seinfeld, J. H. Can chemical effects on cloud droplet number rival the first indirect effect? *Geophys. Res. Lett.* **2002**, *29* (17), 29−1.

(18) Comiso, J. C. A rapidly declining perennial sea ice cover in the Arctic. *Geophys. Res. Lett.* **2002**, *29* (20), 17−1.

(19) Holmes, R. M.; McClelland, J. W.; Peterson, B. J.; Tank, S. E.; Bulygina, E.; Eglinton, T. I.; Gordeev, V. V.; Gurtovaya, T. Y.; Raymond, P. A.; Repeta, D. J.; Staples, R.; Striegl, R. G.; Zhulidov, A. V.; Zimov, S. A. Seasonal and Annual Fluxes of Nutrients and Organic Matter from Large Rivers to the Arctic Ocean and Surrounding Seas. *Estuaries Coasts* **2012**, *35* (2), 369−382.

(20) Aguilar-Islas, A. M.; Rember, R. D.; Mordy, C. W.; Wu, J., Sea ice-derived dissolved iron and its potential influence on the spring algal bloom in the Bering Sea. *Geophys. Res. Lett.* **2008**, *35*, (24).10.1029/2008GL035736

(21) Klunder, M. B.; Bauch, D.; Laan, P.; De Baar, H. J. W.; Van Heuven, S.; Ober, S., Dissolved iron in the Arctic shelf seas and surface waters of the central Arctic Ocean: Impact of Arctic river water and ice-melt. *J. Geophys. Res.* **2012**, *117*, (1).10.1029/2011JC007133

(22) Schwartz, S. E. Mass-transport considerations pertinent to aqueous phase reactions of gases in liquid-water clouds. *Chemistry of Multiphase Atmospheric Systems* **1986**, 415−471.

(23) Allan, J. D.; Topping, D. O.; Good, N.; Irwin, M.; Flynn, M.; Williams, P. I.; Coe, H.; Baker, A. R.; Martino, M.; Niedermeier, N.; Wiedensohler, A.; Lehmann, S.; Müller, K.; Herrmann, H.; McFiggans, G. Composition and properties of atmospheric particles in the eastern Atlantic and impacts on gas phase uptake rates. *Atmos. Chem. Phys.* **2009**, *9* (23), 9299−9314.

(24) Kulmala, M.; Korhonen, P.; Vesala, T.; Hansson, H. C.; Noone, K.; Svenningsson, B. The effect of hygroscopicity on cloud droplet formation. *Tellus, Ser. B* **1996**, *48* (3), 347−360.

(25) Sakurai, H.; Tobias, H. J.; Park, K.; Zarling, D.; Docherty, K. S.; Kittelson, D. B.; McMurry, P. H.; Ziemann, P. J. On-line measurements of diesel nanoparticle composition and volatility. *Atmos. Environ.* **2003**, *37* (9−10), 1199−1210.

(26) Park, K.; Kim, G.; Kim, J. S.; Yoon, Y. J.; Cho, H. J.; Ström, J. Mixing state of size-selected submicrometer particles in the arctic in May and September 2012. *Environ. Sci. Technol.* **2014**, *48* (2), 909−919.

(27) McMurry, P. H.; Kuang, C.; Smith, J. N.; Zhao, J.; Eisele, F. Atmospheric New Particle Formation: Physical and Chemical Measurements. *Aerosol Measurement: Principles, Techniques, and Applications: Third Edition* **2011**, 681−695.

(28) McMurry, P. H.; Fink, M.; Sakurai, H.; Stolzenburg, M. R.; Mauldin, R. L.; Smith, J.; Eisele, F.; Moore, K.; Sjostedt, S.; Tanner, D.; Huey, L. G.; Nowak, J. B.; Edgerton, E.; Voisin, D. A criterion for new particle formation in the sulfur-rich Atlanta atmosphere. *J. Geophys. Res.* **2005**, *110* (22), 1−10.

(29) McMurry, P. H.; Woo, K. S.; Weber, R.; Chen, D. R.; Pui, D. Y. H. Size distributions of 3−10 nm atmospheric particles: Implications for nucleation mechanisms. *Philos. Trans. R. Soc., A* **2000**, *358* (1775), 2625−2642.

(30) Lee, T. K.; Lee, J. H.; Kim, H.; Rim, C. W. Field measurement of local ice pressures on the ARAON in the Beaufort Sea. *Int. J. Nav. Archit. Ocean Eng.* **2014**, *6* (4), 788−799.

(31) Rader, D. J.; McMurry, P. H. Application of the tandem differential mobility analyzer to studies of droplet growth or evaporation. *J. Aerosol Sci.* **1986**, *17* (5), 771−787.

(32) Park, K.; Kim, J. S.; Park, S. H. Measurements of hygroscopicity and volatility of atmospheric ultrafine particles during ultrafine particle formation events at urban, industrial, and coastal sites. *Environ. Sci. Technol.* **2009**, *43* (17), 6710−6716.

(33) Johnson, G. R.; Ristovski, Z. D.; D'Anna, B.; Morawska, L. Hygroscopic behavior of partially volatilized coastal marine aerosols using the volatilization and humidification tandem differential mobility analyzer technique. *J. Geophys. Res.* **2005**, *110* (20), 1−14.

(34) Villani, P.; Picard, D.; Michaud, V.; Laj, P.; Wiedensohler, A. Design and validation of a volatility hygroscopic Tandem Differential Mobility Analyzer (VH-TDMA) to characterize the relationships between the thermal and hygroscopic properties of atmospheric aerosol particles. *Aerosol Sci. Technol.* **2008**, *42* (9), 729−741.

(35) Kim, J. S.; Kim, Y. J.; Park, K. Measurements of hygroscopicity and volatility of atmospheric ultrafine particles in the rural Pearl River Delta area of China. *Atmos. Environ.* **2011**, *45* (27), 4661−4670.

(36) Kim, J.; Maskey, S.; Yoon, Y. J.; Park, K. Mixing state of size-selected submicrometer particles during photochemical and combustion events measured with the tandem system. *Aerosol Sci. Technol.* **2013**, *47* (7), 746−754.

(37) Hermann, M., Development and Application of An Aerosol Measurement System for Use on Commercial Aircraft. Ph.D. Thesis, Univ. Leipzig, Germany, 2000, 1−144.

(38) Alam, A.; Shi, J. P.; Harrison, R. M. Observations of new particle formation in urban air. *J. Geophys. Res.* **2003**, *108*, 3, 10.1029/2001JD001417

(39) Yoon, Y. J.; Ceburnis, D.; Cavalli, F.; Jourdan, O.; Putaud, J. P.; Facchini, M. C.; Decesari, S.; Fuzzi, S.; Sellegri, K.; Jennings, S. G.; O'Dowd, C. D., Seasonal characteristics of the physicochemical properties of North Atlantic marine atmospheric aerosols. *J. Geophys. Res.* **2007**, *112*, (4).10.1029/2005JD007044

(40) O'Dowd, C. D.; Smith, M. H.; Consterdine, I. E.; Lowe, J. A. Marine aerosol, sea-salt, and the marine sulphur cycle: A short review. *Atmos. Environ.* **1997**, *31* (1), 73−80.

(41) Good, N.; Topping, D. O.; Allan, J. D.; Flynn, M.; Fuentes, E.; Irwin, M.; Williams, P. I.; Coe, H.; McFiggans, G. Consistency between parameterisations of aerosol hygroscopicity and CCN activity during the RHaMBLe discovery cruise. *Atmos. Chem. Phys.* **2010**, *10* (7), 3189−3203.

(42) Covert, D. S.; Kapustin, V. N.; Bates, T. S.; Quinn, P. K. Physical properties of marine boundary layer aerosol particles of the mid-Pacific in relation to sources and meteorological transport. *J. Geophys. Res.* **1996**, *101* (D3), 6919−6930.

(43) Hoppel, W. A.; Fitzgerald, J. W.; Frick, G. M.; Larson, R. E.; Mack, E. J. Aerosol size distributions and optical properties found in the marine boundary layer over the Atlantic Ocean. *J. Geophys. Res.* **1990**, *95* (D4), 3659−3686.

(44) Bates, T. S.; Kapustin, V. N.; Quinn, P. K.; Covert, D. S.; Coffman, D. J.; Mari, C.; Durkee, P. A.; De Bruyn, W. J.; Saltzman, E. S. Processes controlling the distribution of aerosol particles in the lower marine boundary layer during the First Aerosol Characterization Experiment (ACE 1). *J. Geophys. Res.* **1998**, *103* (D13), 16369−16383.

(45) Koponen, I. K.; Virkkula, A.; Hillamo, R.; Kerminen, V. M.; Kulmala, M. Number size distributions and concentrations of marine aerosols: Observations during a cruise between the English Channel and the coast of Antarctica. *J. Geophys. Res.* **2002**, *107* (24), 4753.

(46) Yoon, Y. J.; O'Dowd, C. D.; Jennings, S. G.; Lee, S. H. Statistical characteristics and predictability of particle formation events at Mace Head. *J. Geophys. Res.* **2006**, *111* (13), D13204.

(47) O'Dowd, C. D.; De Leeuw, G. Marine aerosol production: A review of the current knowledge. *Philos. Trans. R. Soc., A* **2007**, *365* (1856), 1753−1774.

(48) Modini, R. L.; Ristovski, Z. D.; Johnson, G. R.; He, C.; Surawski, N.; Morawska, L.; Suni, T.; Kulmala, M. New particle formation and growth at a remote, sub-tropical coastal location. *Atmos. Chem. Phys.* **2009**, *9* (19), 7607−7621.

(49) Whitehead, J. D.; McFiggans, G. B.; Gallagher, M. W.; Flynn, M. J. Direct linkage between tidally driven coastal ozone deposition fluxes, particle emission fluxes, and subsequent CCN formation. *Geophys. Res. Lett.* **2009**, *36* (4), L04806.

(50) Heintzenberg, J.; Leck, C.; Birmili, W.; Bigg, E. K. The modal structure of the summer Arctic aerosol and its connection to aerosol processes. *J. Aerosol Sci.* **2004**, *35* (SUPPL. 2), S723−S724.

(51) Raven, J. A.; Richardson, K. *Marine environments. Photosynthesis in Contrasting Environments*; Elsevier Science Publishers: The Hague, 1986; pp 337−396.

(52) Agusti, S.; Enriquez, S.; Frost-Christensen, H.; Sand-Jensen, K.; Duarte, C. M. Light harvesting among photosynthetic organisms. *Funct. Ecol.* **1994**, *8* (2), 273−279.

(53) Uitz, J.; Claustre, H.; Morel, A.; Hooker, S. B., Vertical distribution of phytoplankton communities in open ocean: An assessment based on surface chlorophyll. *J. Geophys. Res.* **2006**, *111*, (8).10.1029/2005JC003207

(54) Van De Poll, W. H.; Kulk, G.; Timmermans, K. R.; Brussaard, C. P. D.; Van Der Woerd, H. J.; Kehoe, M. J.; Mojica, K. D. A.; Visser, R. J. W.; Rozema, P. D.; Buma, A. G. J. Phytoplankton chlorophyll a biomass, composition, and productivity along a temperature and stratification gradient in the northeast Atlantic Ocean. *Biogeosciences* **2013**, *10* (6), 4227−4240.

(55) Gantt, B.; Meskhidze, N. The physical and chemical characteristics of marine primary organic aerosol: A review. *Atmos. Chem. Phys.* **2013**, *13* (8), 3979−3996.

(56) Väkevä, M.; Hämeri, K.; Aalto, P. P., Hygroscopic properties of nucleation mode and Aitken mode particles during nucleation bursts and in background air on the west coast of Ireland. *J. Geophys. Res.* **2002**, *107*, (19).10.1029/2000JD000176

(57) Mäkelä, J. M.; Hoffmann, T.; Holzke, C.; Väkevä, M.; Suni, T.; Mattila, T.; Aalto, P. P.; Tapper, U.; Kauppinen, E. I.; O'Dowd, C. D., Biogenic iodine emissions and identification of end-products in coastal ultrafine particles during nucleation bursts. *J. Geophys. Res.* **2002**, *107*, (19).10.1029/2001JD000580

(58) Vaattovaara, P.; Huttunen, P. E.; Yoon, Y. J.; Joutsensaari, J.; Lehtinen, K. E. J.; O'Dowd, C. D.; Laaksonen, A. The composition of nucleation and Aitken modes particles during coastal nucleation events: Evidence for marine secondary organic contribution. *Atmos. Chem. Phys.* **2006**, *6* (12), 4601−4616.

(59) Allan, J. D.; Williams, P. I.; Najera, J.; Whitehead, J. D.; Flynn, M. J.; Taylor, J. W.; Liu, D.; Darbyshire, E.; Carpenter, L. J.; Chance, R.; Andrews, S. J.; Hackenberg, S. C.; McFiggans, G. Iodine observed in new particle formation events in the Arctic atmosphere during ACCACIA. *Atmos. Chem. Phys.* **2015**, *15* (10), 5599−5609.

(60) Stokes, R. H.; Robinson, R. A. Interactions in aqueous nonelectrolyte solutions. I. Solute-solvent equilibria. *J. Phys. Chem.* **1966**, *70* (7), 2126−2131.

(61) Savoie, D. L.; Arimoto, R.; Keene, W. C.; Prospera, J. M.; Duce, R. A.; Galloway, J. N. Marine biogenic and anthropogenic contributions to non-sea-salt sulfate in the marine boundary layer over the North Atlantic Ocean. *J. Geophys. Res.* **2002**, *107* (18), 3-1−3-21.

(62) Savoie, D. L.; Prospero, J. M. Comparison of oceanic and continental sources of non-sea-salt sulphate over the Pacific Ocean. *Nature* **1989**, *339* (6227), 685−687.

(63) Russell, K. M.; Keene, W. C.; Maben, J. R.; Galloway, J. N.; Moody, J. L. Phase partitioning and dry deposition of atmospheric nitrogen at the mid-Atlantic U.S. coast. *J. Geophys. Res.* **2003**, *108* (21), 1−16.

(64) Murphy, S.; Agrawal, H.; Sorooshian, A.; Padró, L. T.; Gates, H.; Hersey, S.; Welch, W. A.; Jung, H.; Miller, J. W.; Cocker Iii, D. R.; Nenes, A.; Jonsson, H. H.; Flagan, R. C.; Seinfeld, J. H. Comprehensive simultaneous shipboard and airborne characterization of exhaust from a modern container ship at sea. *Environ. Sci. Technol.* **2009**, *43* (13), 4626−4640.

(65) Painemal, D.; Minnis, P.; Nordeen, M. Aerosol variability, synoptic-scale processes, and their link to the cloud microphysics over the northeast Pacific during MAGIC. *J. Geophys. Res., D: Atmos.* **2015**, *120* (10), 5122−5139.